# Design and calibration of a Flush Air Data System (FADS) for prediction of the atmospheric properties during re-entry

**Professor Olivier P. Chazot**

**Von Karman Institute for Fluid Dynamics (VKI)**
**72 Chaussee de Waterloo**
**Rhode-Saint-Genese  1640  Belgium**

Report Date: January 2013

Final Report from 01 October 2011 to 30 September 2012

**Air Force Research Laboratory**
**Air Force Office of Scientific Research**
**European Office of Aerospace Research and Development**
**Unit 4515 Box 14, APO AE 09421**

# REPORT DOCUMENTATION PAGE

Form Approved OMB No. 0704-0188

Public reporting burden for this collection of information is estimated to average 1 hour per response, including the time for reviewing instructions, searching existing data sources, gathering and maintaining the data needed, and completing and reviewing the collection of information. Send comments regarding this burden estimate or any other aspect of this collection of information, including suggestions for reducing the burden, to Department of Defense, Washington Headquarters Services, Directorate for Information Operations and Reports (0704-0188), 1215 Jefferson Davis Highway, Suite 1204, Arlington, VA 22202-4302. Respondents should be aware that notwithstanding any other provision of law, no person shall be subject to any penalty for failing to comply with a collection of information if it does not display a currently valid OMB control number.
**PLEASE DO NOT RETURN YOUR FORM TO THE ABOVE ADDRESS.**

| 1. REPORT DATE *(DD-MM-YYYY)* | 2. REPORT TYPE | 3. DATES COVERED *(From – To)* |
|---|---|---|
| 3 January 2013 | Final Report | 1 October 2011 – 30 September 2012 |

**4. TITLE AND SUBTITLE**

**Design and calibration of a Flush Air Data System (FADS) for prediction of the atmospheric properties during re-entry**

**5a. CONTRACT NUMBER**

FA8655-11-1-3079

**5b. GRANT NUMBER**

**Grant 11-3079**

**5c. PROGRAM ELEMENT NUMBER**

61102F

**6. AUTHOR(S)**

Professor Olivier P. Chazot

**5d. PROJECT NUMBER**

**5d. TASK NUMBER**

**5e. WORK UNIT NUMBER**

**7. PERFORMING ORGANIZATION NAME(S) AND ADDRESS(ES)**

Von Karman Institute for Fluid Dynamics (VKI)
72 Chaussee de Waterloo
Rhode-Saint-Genese 1640 Belgium

**8. PERFORMING ORGANIZATION REPORT NUMBER**

N/A

**9. SPONSORING/MONITORING AGENCY NAME(S) AND ADDRESS(ES)**

EOARD
Unit 4515 BOX 14
APO AE 09421

**10. SPONSOR/MONITOR'S ACRONYM(S)**

AFRL/AFOSR/IOE (EOARD)

**11. SPONSOR/MONITOR'S REPORT NUMBER(S)**

**AFRL-AFOSR-UK-TR-2013-0006**

**12. DISTRIBUTION/AVAILABILITY STATEMENT**

Approved for public release; distribution is unlimited. (approval given by local Public Affairs Office)

**13. SUPPLEMENTARY NOTES**

**14. ABSTRACT**

In this effort was developed a high temperature 1-D solver to reconstruct the Longshot wind tunnel conditions. It supports calorically imperfect, thermally perfect flows in thermal equilibrium or non-equilibrium. For non-equilibrium in the Longshot, the vibrational temperature has to be imposed. A prediction was obtained by solving Vibrational-Translational Energy Transfer and energy conservation equations for the Longshot nozzle geometry. Compared to the traditional rebuilding method, thermal non-equilibrium has a strong effect on the reconstructed density and Mach number of up to 6% and 4% respectively. Caloric imperfection had a more limited effect of up to 1% and 0,4% respectively. These results indicate that better understanding of thermal non-equilibrium due to the strong nozzle expansion is required to use the wind tunnel as a FADS calibration tool. Specifically, prior knowledge of the vibrational temperature is required. Caloric imperfections need to be taken into account to reconstruct the flow conditions as well, but this requires no prior knowledge.

**15. SUBJECT TERMS**

EOARD, Instrumentation, Hypersonics, FADS, Flush Air Data System, Atmospheric Re-entry

| 16. SECURITY CLASSIFICATION OF: | | | 17. LIMITATION OF ABSTRACT | 18, NUMBER OF PAGES | 19a. NAME OF RESPONSIBLE PERSON |
|---|---|---|---|---|---|
| **a. REPORT** UNCLAS | **b. ABSTRACT** UNCLAS | **c. THIS PAGE** UNCLAS | SAR | 28 | Gregg Abate |
| | | | | | **19b. TELEPHONE NUMBER** *(Include area code)* +44 (0)1895 616021 |

**Standard Form 298** (Rev. 8/98)
Prescribed by ANSI Std. Z39-18

# Design and calibration of a Flush Air Data System (FADS) for prediction of the atmospheric properties during re-entry

Final Report submitted to

Dr. Gregg L. Abate

Chief, Aeronautical Sciences

European Office of Aerospace Research and Development (EOARD)

United States Air Force Research Laboratory (AFRL)

1 December 2012

by

Director Jean Muylaert (P.I.)

von Karman Institute for Fluid Dynamics

Chaussée de Waterloo 72, 1640 Rhode-St-Genèse, Belgium

Phone: +32 2 359 96 01    Fax: +32 2 359 96 00   Email: jean.muylaert@gmail.com

# I.   Table of contents

# II. Introduction

Determination of the atmospheric properties during Earth re-entry is crucial, in particular, accurate knowledge of the free stream density is required for vehicle control, reaching a landing site, predicting peak heating and characterizing fluid dynamical phenomena on spacecraft. Better tools need to be developed to determine the free stream density and to accurately quantify its uncertainty. Reduction of the error bars on heat flux and drag coefficient predictions in both real flight and ground test facilities is deemed to be necessary for the development of hypersonic flight on Earth. Atmospheric density profiles have been obtained by lidars, balloon drop tests, tracking ejected spheres or in-situ from sounding rocket flights or derived from classical air data systems. These methods have their limits and/or require accurate knowledge of the aerodynamic characteristics of the vehicle. The uncertainty on the free stream conditions is thus mixed with that on the aerodynamics. Additionally, sounding missions poorly represent instantaneous conditions encountered in flight.
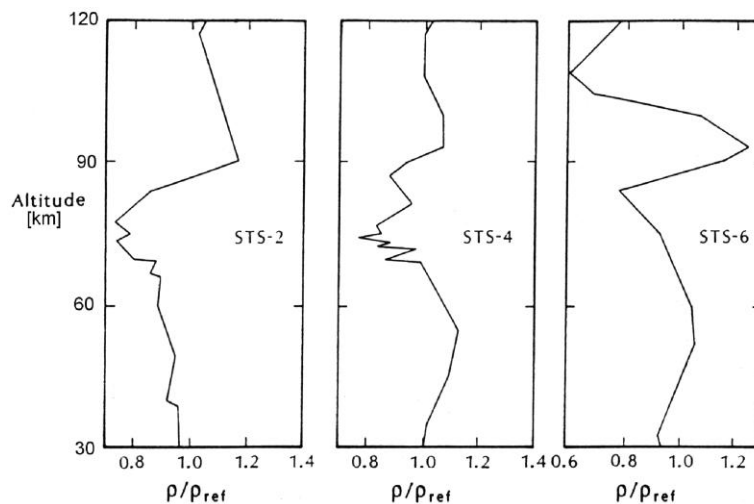


**Fig. 1 Shuttle-derived densities compared to the 1962 U.S. standard atmosphere [ref. 7].**

In Fig. 1, the densities obtained during Space Shuttle re-entry are seen to deviate up to 20% from the standard atmosphere. These deviations can reach extreme values as large as 80% over vertical distances of a few kilometers [Ref. 1]. Sounding rocket missions usually rely on falling spheres to determine density. This geometry is used because drag is the principal aerodynamic force [Ref. 2]. Sphere velocity and acceleration are measured by accelerometers or radar link. If the drag coefficient is known, the density can be simply derived. The drag coefficient depends strongly on the Mach and Reynolds numbers and is not accurately known throughout the entire

3

flight regime [Ref. 2]. At high altitudes, the error on the derived density can exceed 20% as shown in Fig. 2.

In the same vein as the falling sphere experiments, combining position and velocity of a vehicle during entry with the drag coefficient, the density can be derived in-situ. The drag coefficient depends on the vehicle attitude and velocity, free stream conditions and gas thermochemistry. This quantity is established mainly in ground testing facilities and by means of computational fluid dynamics calculations. These can suffer from limited flight representation, poor flow characterization and high or even unknown uncertainties. Even if position and velocity are perfectly determined in-flight, the uncertainty on the calculated density is conflated with that on the vehicle aerodynamics.
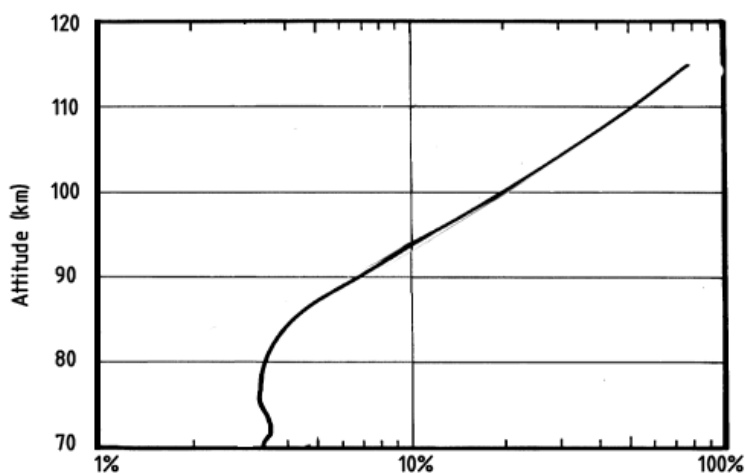


Fig. 2 Uncertainty on density derived from falling spheres [Ref. 7]

We propose to develop and validate a new approach to determine the free stream density using a Flush Air Data System (FADS) that uses a combination of Pitot-static pressure measurements with calorimetric heat flux measurements integrated on 5 locations in the nose region. The purpose of the present grant is to develop and validate the transfer function that relates these 5 pressure- and 5 heat flux measurements with the free stream density. Commonly, a calorically perfect gas model is used for such a calculation, leading to significant errors that arise from the high-temperature gas effects in the hypersonic flight regime. The new approach that we propose will be more accurate than the conventional models as real gas (high temperature) effects will be taken into account. In the future these transfer functions could not only be used for correct reconstruction of the aerothermodynamic characterization of re-entry flight vehicles but could also be used for real-time density and speed vector rebuilding serving flight control loops. The quantification of the influence of uncertainty on the physical system, also referred to as Uncertainty Quantification (UQ), will allow to properly predict the system response to random inputs due to experimental error and physico-chemical model uncertainty, in particular by using inverse problem methods [Ref. 3].

# III. Technical approach

The final objective is to provide a FADS transfer function accounting for high-temperature effects and taking into account experimental and numerical uncertainty, thus leading to distinctly improved results as compared to conventional techniques [Ref.3].

## Longshot flow rebuilding

The validity of this new FADS method can be assessed in the VKI Longshot hypersonic wind tunnel for the moderate altitude regime. For this the wind tunnel flow must be accurately characterized, i.e. accurate rebuilding of the tunnel free stream conditions is required. The main limitation in the traditional Longshot flow rebuilding, is the assumption of a calorically perfect flow. In reality, the thermal flow properties are expected to change through the shock wave. We have developed a 1-D data rebuilding program based on the VKI developed Mutation code [Ref. 5,6,7], that models high-temperature effects and thermal non-equilibrium for pure gases or mixtures. We also attempt to measure additional conditions to better constrain the tunnel flow conditions.

## FADS methodology

To assemble a FADS transfer function, we relied on the modified Newtonian flow model to predict the surface pressure distribution from total pressure, Mach number and airflow angles. Its main assumption is that of a calorically perfect flow. We can address this limitation using the 1-D flow solver supporting high temperature effects.

To utilize surface pressure measurements to predict flow conditions, the forward pressure model must be inverted. For this purpose, we have implemented a least squares inversion algorithm. We subjected it to tests on synthetic data and wind tunnel pressure distributions.

## Wind tunnel testing

We have manufactured a generic blunt body probe, equipped with four pressure and four temperature (heat flux) sensors. It is currently being tested in the Longshot wind tunnel at Mach 14. We test the ability of the least squares solver to retrieve the flow conditions. By varying the attitude of the blunt body, a relationship between the airflow angles and the heat flux distribution could be observed.
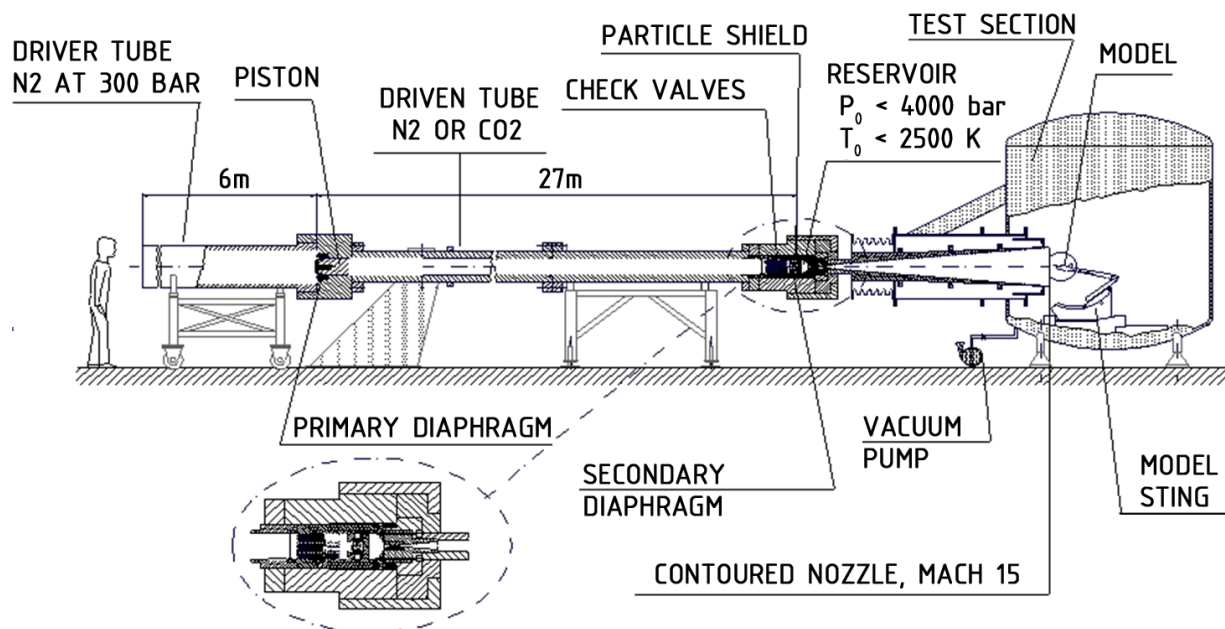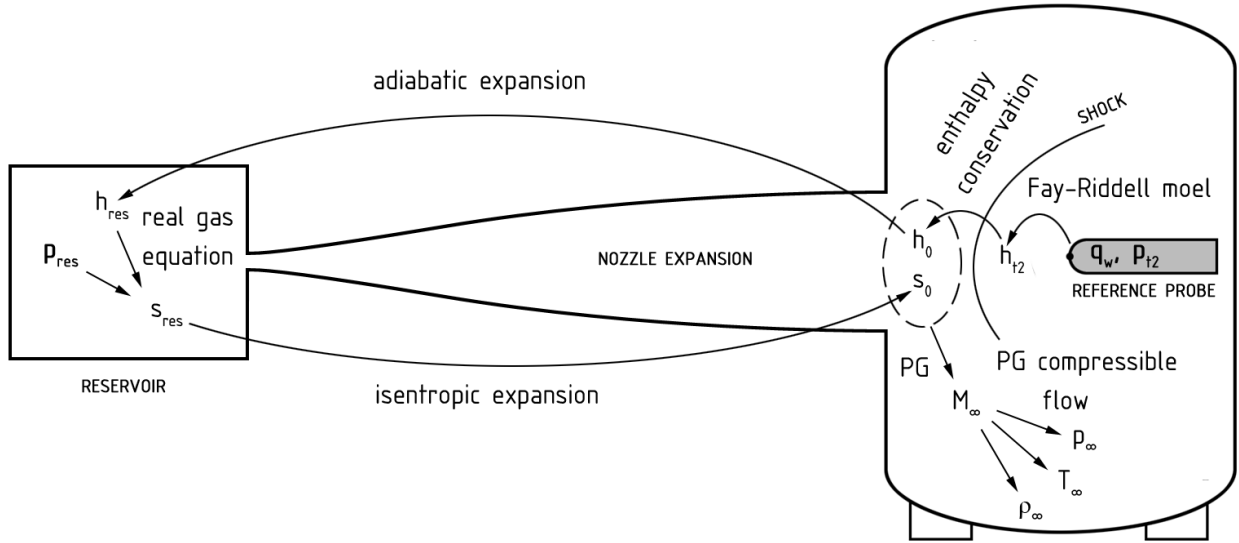
# 1. Longshot flow rebuilding



**Fig. 3 VKI Longshot hypersonic piston gun tunnel**

| Reynolds | $p_0$ | $T_0$ | $M_\infty$ | $Re_\infty$ | $p_\infty$ | $T_\infty$ |
|---|---|---|---|---|---|---|
| | bar | K | - | 1/m | Pa | K |
| low | 1400 | 2300 | 15 | 10 .106 | 280 | 50 |
| med | 3400 | 2300 | 15 | 20 .106 | 460 | 50 |
| high | 4500 | 2300 | 15 | 25 .106 | 550 | 50 |

**Table 1 Typical Longshot conditions at start of test (1 ms)**

The VKI Longshot operates at Mach 14 with nitrogen or carbon dioxide (Fig. 3 and Tab. 1). It is a short duration tunnel with very limited high temperature effects. The standard rebuilding procedure relies on routine stagnation point and tunnel reservoir measurements. From the stagnation pressure, stagnation heat flux and reservoir pressure, all of the tunnel flow conditions are derived. The procedure is shown schematically in Fig. 4, a detailed flow chart is provided in the Appendix. This calculation relies on a Fay-Riddell heat flux model, calorically perfect gas equations, conservation of entropy and enthalpy during the nozzle expansion, and an empirical equation of state for calculating enthalpies at high temperature and/or pressure conditions. Note that although high temperature effects are included in enthalpy calculations at the stagnation point and reservoir, the tunnel flow conditions are based on calorically perfect gas equations where $\gamma = c_p/c_v$ = 1.4 for nitrogen.

6

**Fig. 4 Traditional Longshot flow rebuilding (calorically perfect free stream)**

To significantly increase the accuracy of the flow rebuilding, we update both our analytical tools and flow measurements. We have developed a 1-D tunnel flow solver that supports high temperature and thermal non-equilibrium effects. We have also manufactured a static pressure probe, as a direct free stream measurement removes the need for reservoir and expansion modeling.

## High temperature 1-D solver

A gas in the process of being slowed down is heated due to the kinetic energy of flow. The amount of the heating depends on the specific heat capacity of the gas. If the specific heat capacity is a constant value, the gas is said to be calorically perfect and if the specific heat capacity changes, the gas is said to be *calorically imperfect*. At fairly high Mach numbers and temperatures such as in Longshot, the gas is calorically imperfect. However, it still follows the ideal gas equation of state given the appropriate (high temperature) gas constants. At even higher Mach numbers and temperatures, gas molecules will break up and the ideal equation of state is not valid anymore. In that case, the gas is said to be *thermally imperfect* as well. The 1-D solver described here supports calorically imperfect but not thermally imperfect flows. Temperatures in the Longshot are sufficiently low for nitrogen to remain thermally perfect. Finally, the solver supports *thermal non-equilibrium*, meaning that the temperatures of the various modes (translational, vibrational, electronic…) are not required to be equal.

The routine solves for the tunnel flow conditions starting from the stagnation pressure, stagnation heat flux and reservoir pressure, like the traditional calorically perfect rebuilding routine. More specifically, the Rankine-Hugoniot or shock conservation equations are solved iteratively:

$$\rho_1 v_1 = \rho_2 v_2$$

7

$$p_1 + \rho_1 v_1^2 = p_2 + \rho_2 v_2^2$$

$$(\rho_2 E_2 + p_2)v_2 = (\rho_1 E_1 + p_1)v_1$$

Where the total energy E equals the internal energy *e* plus a kinetic energy term:

$$E = e + \frac{1}{2}v^2$$

The internal energy is calculated by means of *Statistical Thermodynamics for High-Temperature gases* described in [Ref. 5,6,7]. The internal energy of each species is calculated as the sum of the translation, electronic, rotation, vibrational and formation energies. As such, high temperature or real gas effects are incorporated.

The iterative solver consists of a standard least squares solver for non-linear problems, similar to the one that will be described below. By accurately calculating the internal energies and deriving flow properties such as the heat capacity ratio and speed of sound from them:

$$\gamma = \frac{\partial h}{\partial e}$$

$$a_1 = \sqrt{\gamma / \frac{\partial \rho_1}{\partial p_1}}$$

Where $h$ is the specific enthalpy and $a_1$ the sound velocity. The sought after tunnel flow conditions such as the Mach number can then be calculated:

$$M_1 = \frac{v_1}{a_1}$$

In the Longshot wind tunnel, vibrational non-equilibrium $T_{V1} \neq T_1$ is expected after the nozzle expansion, while temperatures are too low for electronic excitation. After the shock wave, thermal equilibrium can be assumed. While the solver allows for the inclusion of thermal non-equilibrium by setting $T_{V1}$, the actual value of the vibrational temperature in the free stream is unknown. To predict $T_{V1}$ after the vibrational mode has been frozen in the nozzle expansion, the following system of equations was solved by a 1-D CFD code:

$$\rho E = \rho e + \frac{1}{2}\rho v^2 \qquad\qquad \text{Total energy}$$

$$\rho H = \rho E + p \qquad\qquad \text{Total enthalpy}$$

$$\Omega^{VT} = \rho \frac{e^V(T) - e^V(T^V)}{\tau^{VT}} \qquad\qquad \text{Vibrational-Translational Energy Transfer}$$

$$\frac{\partial U}{\partial t} + \frac{\partial F}{\partial x} = \Omega - \frac{d\ln(A)}{dx}G \qquad\qquad \text{Energy conservation}$$

8

$$U = [\; \rho \;\; \rho u \;\; \rho E \;\; \rho e^V \;]^T$$

$$F = [\; \rho u \;\; p + \rho u^2 \;\; \rho u H \;\; \rho u e^V \;]^T$$

$$G = [\; \rho u \;\; \rho u^2 \;\; \rho u H \;\; \rho u e^V \;]^T$$

$$\Omega = [\; 0 \;\; 0 \;\; 0 \;\; \Omega^{VT} \;]^T$$

Resulting in the prediction a vibrational temperature frozen at about 1350 K, compared to a much lower static temperature of about 50 K:
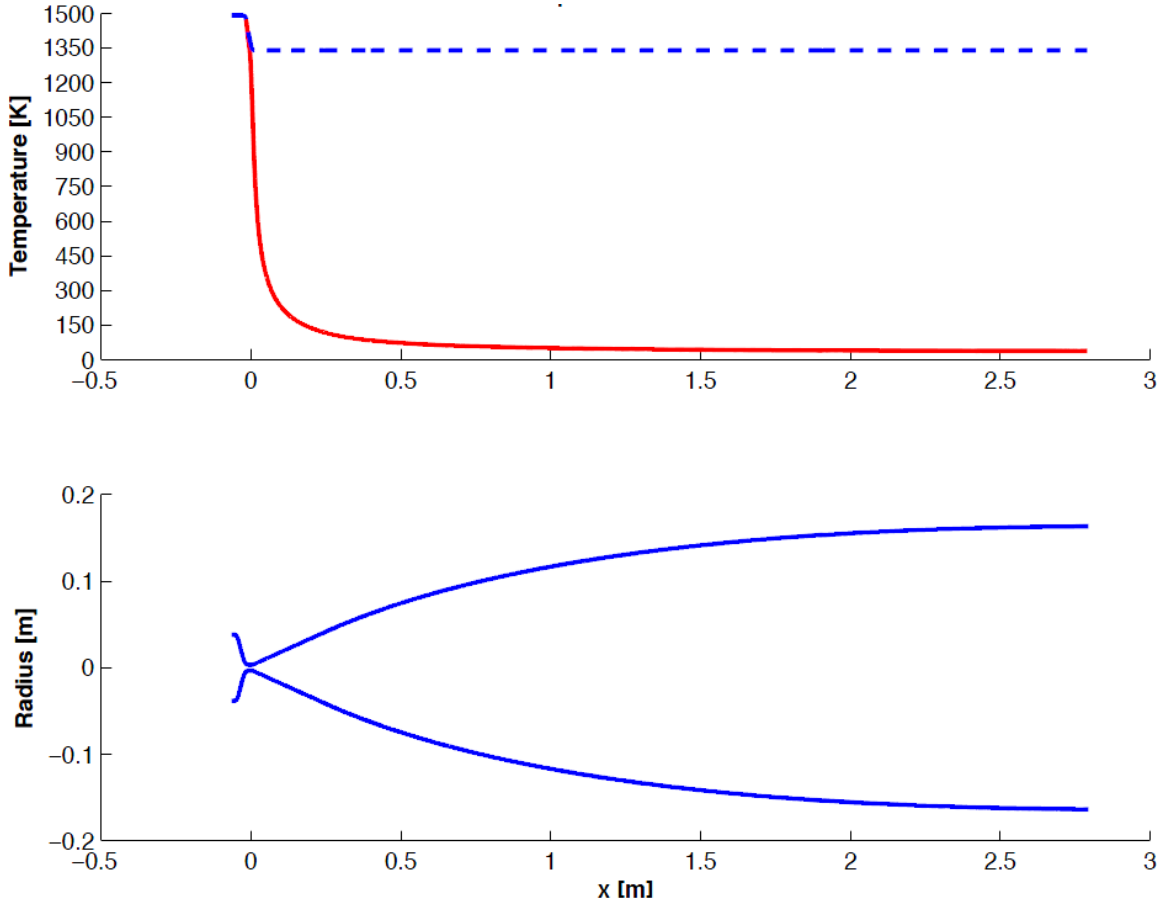


**Fig. 5 Above: static temperature $T_1$ (red) and vibrational temperature $T_{v1}$ (blue dashed)**
**Fig. 5 Below: nozzle radius versus distance from throat**

## Nagamatsu static pressure probe

The uncertainty on the derived tunnel flow conditions can be significantly reduced by measuring a free stream condition directly. This way, no reservoir modeling or nozzle expansion idealization is required. However, the free stream conditions are very small compared to the stagnation conditions and are thus hard to measure with intrusive probes. The static pressure for example amounts to a few hundred Pascal compared to a 100 kPa stagnation pressure.

9
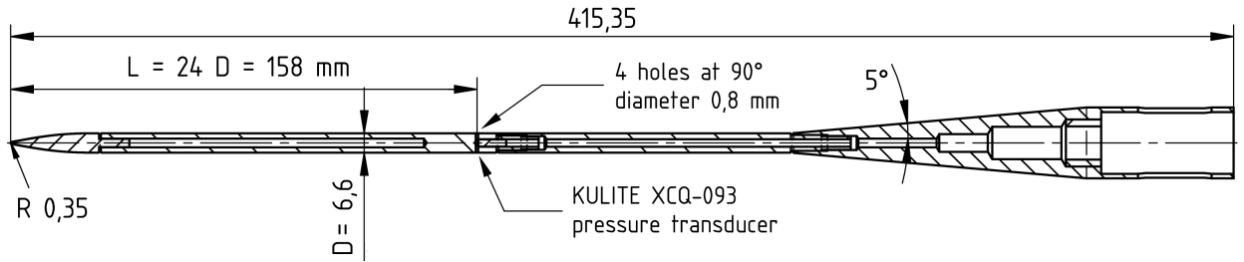
**Fig. 6 Single sensor static pressure 'Nagamatsu' probe**

Recently, a static pressure 'Nagamatsu' probe [Ref. 8] was built at VKI (Fig. 6). The slender probe with a contoured nose is designed to produce the least possible amount of flow perturbation. The length-to-diameter ratio L/D of its single pressure sensor position was chosen based on perfect gas 2-D axi-symmetric Navier-Stokes computations (Fig. 7). The pressure at the measurement location should correspond to the free stream static pressure within 5%, while leaving sufficient distance from the back support recirculation bubble. The single sensor Nagamatsu probe reported much higher than expected static pressures (Fig. 8), warranting deeper investigation.
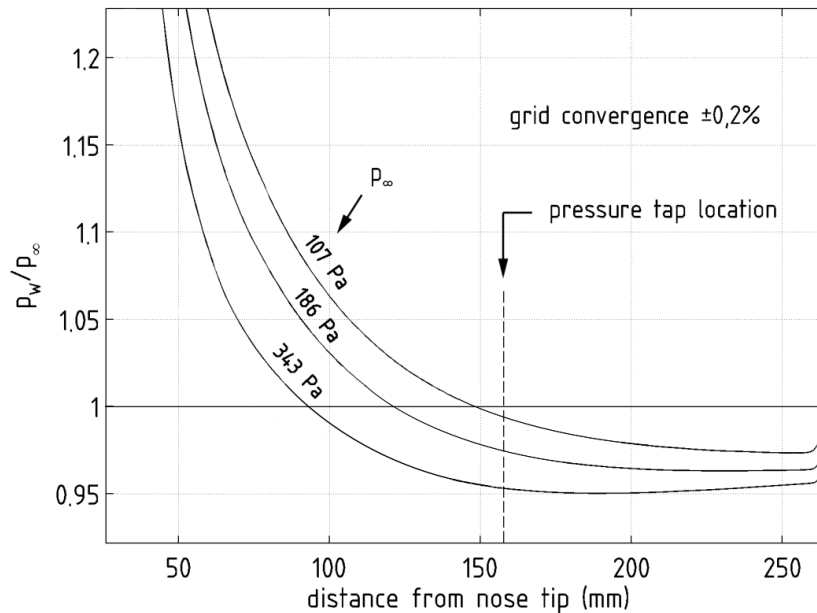


**Fig. 7 Perfect gas CFD for pressure distribution on static pressure 'Nagamatsu' probe**

10
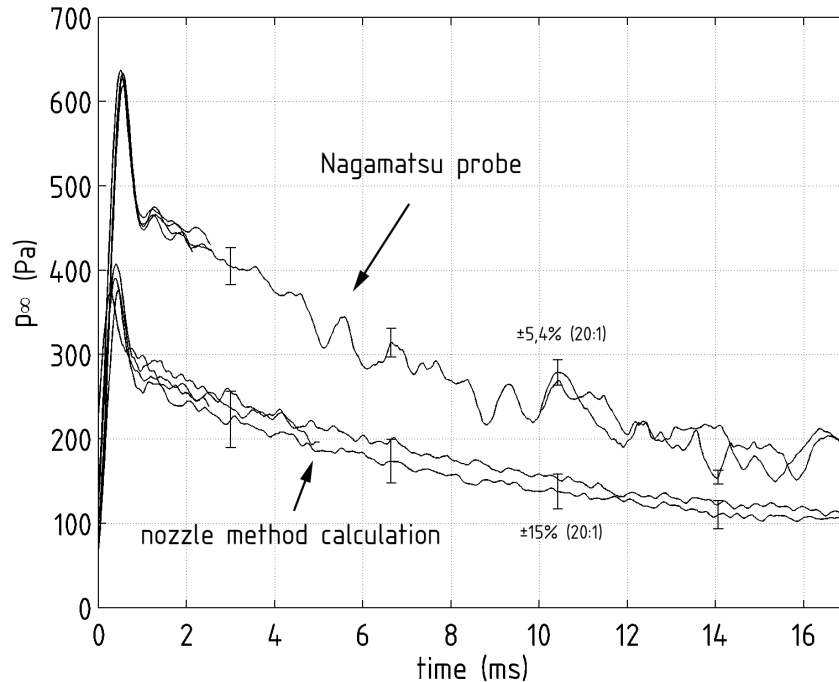
**Fig. 8 Higher than expected static pressure reported by single sensor 'Nagamatsu' probe**

To validate the single sensor measurements, a multi-sensor Nagamatsu probe was developed and built in the present grant (Fig. 9). Compared to the single sensor probe, it has been scaled up by a factor of 1.21. It contains three KULITE XCQ-062 absolute pressure sensors, the middle of which is at the same L/D location as the single sensor on the original probe. Multiple sensors should permit us to observe the pressure distribution on the probe surface and obtain a reliable static pressure measurement. By obtaining direct information on the free stream conditions, the flow rebuilding can be validated or improved. The probe has been manufactured and verified to be leak-free, but has not been tested yet due to technical delays.
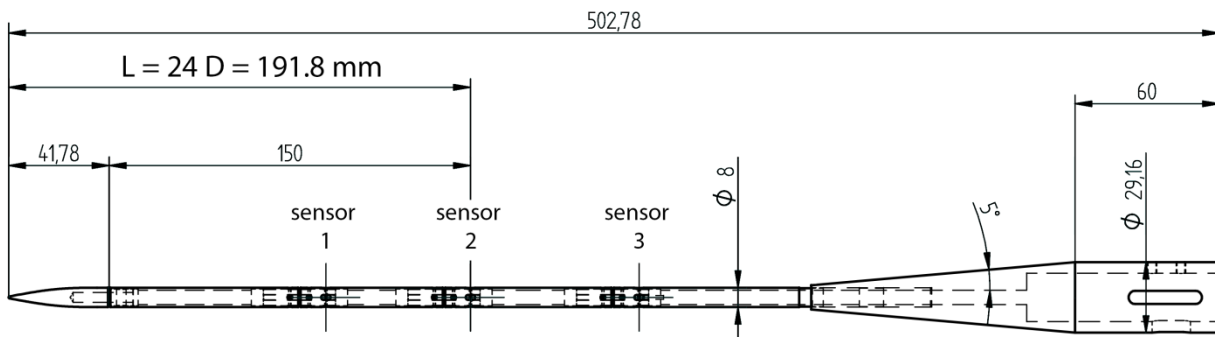


**Fig. 9 Multi-sensor static pressure 'Nagamatsu' probe**

11

## 2. FADS methodology

Classical FADS systems consist of a forward pressure model and an inversion method. The forward model predicts surface pressure distributions from airflow angles and free stream conditions, the inversion method retrieves airflow and free stream conditions from measured pressure distributions. We rely on the modified Newtonian flow model as a basic forward pressure model [Ref. 9]:

$$p_i = p_t[(1 - R)\cos^2\theta_i + R]$$

$$R = \frac{p_\infty}{p_t} = \left[\frac{2}{(\gamma + 1)M_\infty^2}\right]^{\gamma/(\gamma-1)}\left[\frac{2\gamma M_\infty^2 - (\gamma - 1)}{\gamma + 1}\right]^{1/(\gamma-1)}$$

Where $\theta$ depends on airflow angles and cone $\lambda$ and clock $\phi$ angles of the pressure tap locations:

$$\cos\theta_i = \cos\alpha\cos\beta\cos\lambda_i + \sin\beta\sin\phi_i\sin\lambda_i + \sin\alpha\cos\beta\cos\phi_i\sin\lambda_i$$

The density can be retrieved from the dynamic pressure and the velocity. The velocity must be obtained independently in a FADS system. The dynamic pressure is related to the above conditions by

$$q_\infty = p_t\frac{\gamma R M_\infty^2}{2}$$

Limitations of the modified Newtonian pressure model:

- Predicts air flow angles and upstream conditions based on surface pressures only
- Assumes calorically perfect flow (no high temperature effects)
- Surface pressure distribution not affected by shock wave
- Only valid at high Mach numbers

The final two points are of small importance for hypersonic flow over a blunt body. To improve on the calorically perfect flow, the data rebuilding program including high-temperature effects can be used to predict $R$, the pressure ratio across the shock. This leaves the inclusion of heat flux measurements.

A forward prediction of stagnation point heat flux from upstream conditions depends on many thermochemical and –physical conditions, as well as on the wall temperature [Ref. 10]. Stagnation point heat flux can be predicted using the Fay-Riddell model. In real flight condition, an accurate forward prediction of the heat flux is not easily obtained due to limited knowledge of all the required conditions. For the time being, we will investigate whether a useful relationship between the airflow angles and the relative heat flux distribution can be retrieved experimentally.

## Inversion method: Least Squares Solver

We implemented the forward pressure model in MATLAB. To solve it inversely, that is retrieving flow conditions and airflow angles from a measured pressure distribution, we chose to implement a least squares solving routine. This solver is relatively easy to implement and not uncommon for FADS applications [Ref. 11-12].

For a constant heat capacity ratio, the forward pressure model can be written as

$$\boldsymbol{p}_w = f(\boldsymbol{\lambda}, \boldsymbol{\phi}, \alpha, \beta, M_\infty, p_t)$$

Where $\boldsymbol{p}_w$ is a vector containing the surface pressures at the pressure tap locations. Here the airflow angles, Mach number and total pressure are the sought after variables. Either the Mach number or total pressure could be replaced by the static or dynamic pressure, resulting in mathematically equivalent expressions but not necessarily the same numerical conditioning. The Mach number and static pressure have the poorest conditioning, because they depend only on the off-stagnation-point measurements and are several orders of magnitude smaller than the total and dynamic pressures. We have chosen the total pressure for its good conditioning, and the Mach number because we expect it to be known more accurately in the wind tunnel than the static pressure. From the total pressure and Mach number, the dynamic pressure can be derived according to the equations presented before.

Given at least five pressure sensors, this system with four unknowns is over determined but can be inversely solved in a least squares way. The function $f$ is non-linear so an iterative procedure is required. It consists of updating the state vector $\boldsymbol{q} = [\alpha \ \beta \ M_\infty \ p_t]$ until convergence is achieved:

$$\boldsymbol{q}^{k+1} = \boldsymbol{q}^k + \delta\boldsymbol{q}$$

To evaluate the value of the state vector increment, we may write

$$\boldsymbol{b} = \mathbf{J}\,\delta\boldsymbol{q}$$

Where the residual vector $\boldsymbol{b} = \boldsymbol{p}_{w,data} - f(\boldsymbol{q}^k)$ and $\mathbf{J}$ the Jacobian of the pressure model containing first order derivatives at the current state estimate $\boldsymbol{q}^k$ :

$$\mathbf{J} = \begin{bmatrix} \dfrac{\partial p_{w1}}{\partial \alpha} & \dfrac{\partial p_{w1}}{\partial \beta} & \dfrac{\partial p_{w1}}{\partial M_\infty} & \dfrac{\partial p_{w1}}{\partial p_t} \\ \vdots & \vdots & \vdots & \vdots \\ \dfrac{\partial p_{w5}}{\partial \alpha} & \dfrac{\partial p_{w5}}{\partial \beta} & \dfrac{\partial p_{w5}}{\partial M_\infty} & \dfrac{\partial p_{w5}}{\partial p_t} \end{bmatrix}_{\boldsymbol{q}=\boldsymbol{q}^k}$$

The derivatives of the non-linear function $f$ that produces $\boldsymbol{p}_w$ are calculated numerically, using first order forward step differentiation. The state vector increment is obtained by calculating the

13

pseudoinverse of the Jacobian matrix, using the built-in MATLAB function *pinv* that computes the Moore-Penrose pseudoinverse matrix:

$$\delta \boldsymbol{q} = \mathbf{J}^{-1} \boldsymbol{b}$$

Starting from an initial guess $\boldsymbol{q}_0$, the iterative procedure continues until a convergence criterion is met in a chosen number of consecutive iterations. We found that the most robust criterion is that of the maximum relative change of the Euclidian magnitude of the normalized state vector increment:

$$\frac{S^{k+1} - S^k}{S^k} \; < \; \varepsilon$$

$$\text{with} \quad S^k = \left| \frac{\delta q^k}{q^k} \right|^2$$

Where $\varepsilon$ can be set to values as low as $10^{-6}$ and the convergence criterion had to be met for about five iterations. The solver convergence was found to benefit significantly by damping the state increments of the Mach number by a factor between 100 and 1000. This prevents the poorly conditioned Mach number from diverging before the total pressure converges to its optimal estimate.

## 3. Wind tunnel testing
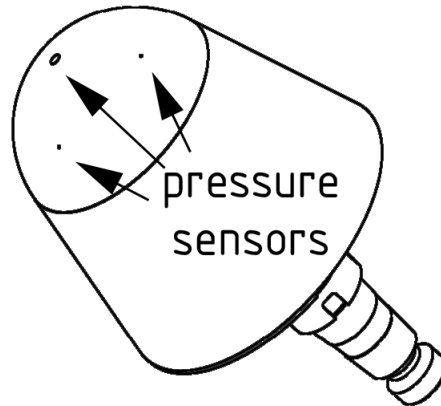


**Fig. 10 Blunt model for validation of the FADS methodology [Ref. 6].**

To facilitate numerical reconstruction, a generic spherical nose probe was be constructed (Fig. 10). It is equipped with sensors simulating the flight RAFLEX sensors as used on the EXPERT flight model. Five combined pressure and temperature transducers were used for the wind tunnel model; one at stagnation and four located at 45° from the stagnation point, distributed evenly around the nose. Experiments in the Longshot are being performed at zero and non–zero angle of attack. The experimental data should serve to validate the FADS transfer function at Mach 14.

14

The established methodology can also be used later in high enthalpy facilities such as the TH2 (RWTH at Aachen, Germany) and other collaborating European or US institutions.

| Test | $\alpha$ | $\beta$ | $\alpha_T$ | $\phi$ |
|------|-----|-----|------|-----|
| 1 | 0 | 0 | 0 | 45 |
| 2 | 0 | 0 | 0 | 0 |
| 3 | 0 | 0 | 0 | 0 |
| 4 | 0 | 0 | 0 | 180 |
| 5 | 5 | 0 | 5 | 0 |
| 6 | 10 | 0 | 10 | 0 |
| 7 | 0 | 10 | 10 | 0 |
| 8 | 7 | 3.5 | 7.5 | 0 |
| 9 | 7 | 7.2 | 10 | 0 |
| 10 | 7 | 3.5 | 7.5 | 0 |
| 11 | 5 | 0 | 5 | 0 |
| 12 | 5 | 0 | 5 | 0 |

**Table 2 Test matrix of the blunt probe in Longshot wind tunnel**

The test matrix (Tab. 2) was constructed to both verify the experimental setup and cover a reasonable range of flow angles. In tests 1-4, the model faces the flow head-on to check repeatability. In test 4 the model is flipped upside down (roll angle 180º) to verify flow and probe alignment. After that, angle of attack and sideslip are varied both separately (tests 5-7) and together (tests 8-10). Finally, repeatability at positive total angle of attack is checked in tests 11-12. At all times, the total angle of attack is one of only four almost equally spaced (Fig. 11).
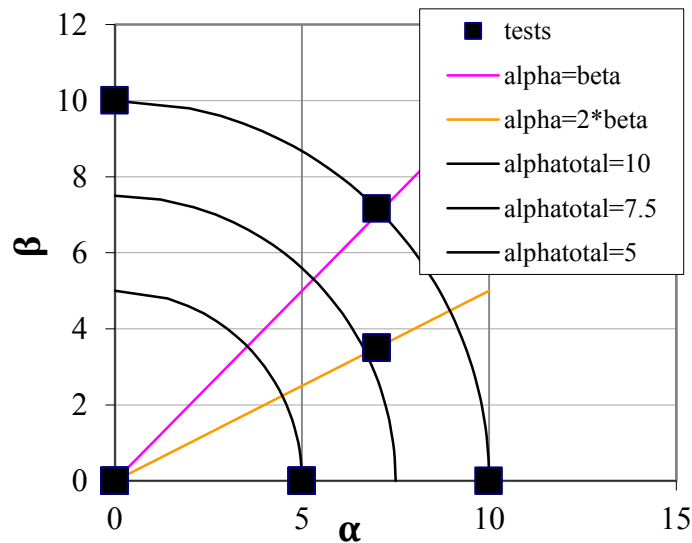


**Fig. 11 Graphical representation of test matrix with iso total-angle-of-attack lines**

15

# IV. Results

## 4. Longshot flow rebuilding

We compared the results of the high temperature 1-D solver (calorically imperfect) to the classical wind tunnel rebuilding routine (calorically perfect). The top graphs (Fig. 12-13) show the calorically imperfect results for free stream density and Mach number. These solutions were obtained by imposing the non-equilibrium vibrational temperature predicted above. The bottom graphs show the percentage deviation of the thermal equilibrium / calorically imperfect (blue) and the thermal equilibrium / calorically perfect (red dashed) from the top solution.
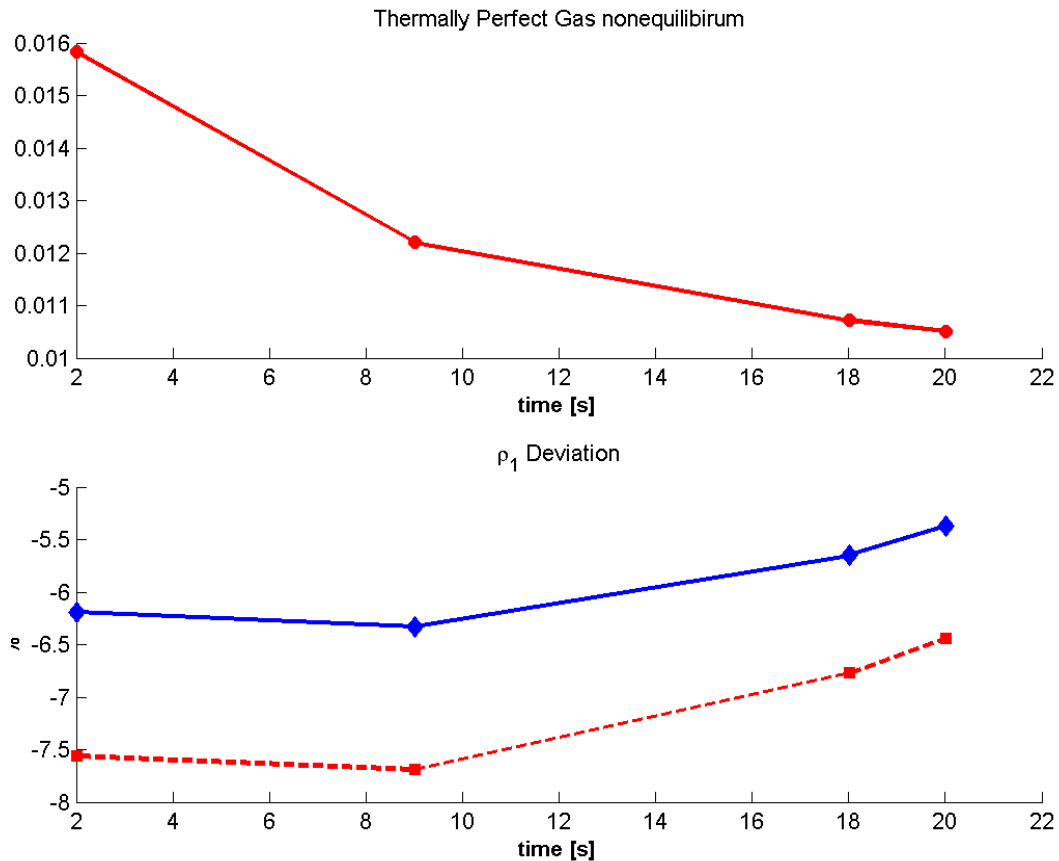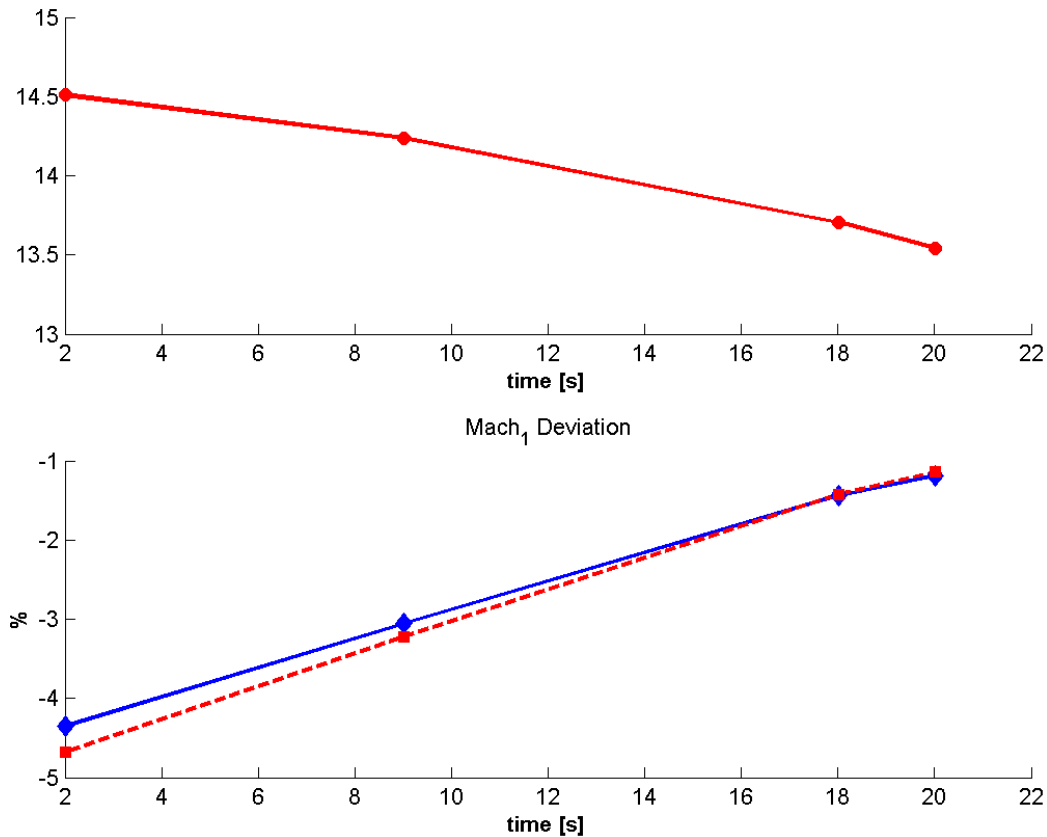


**Fig. 12 various reconstructions of the free stream density**
**Top: TP NEQ / Bottom: TP EQ (blue) and CP EQ (red dashed), percentage deviations**

16

**Fig. 13 various reconstructions of the free stream Mach number**
**Top: TP NEQ / Bottom: TP EQ (blue) and CP EQ (red dashed), percentage deviations**

Thermal non-equilibrium has a very strong effect on the reconstructed tunnel flow conditions, up to 6% for the density and 4% for the Mach number. Caloric imperfections result in an additional 1% change in density and less than 0,5% in Mach number. All deviations decrease as the wind tunnel test progresses, because as the reservoir empties, total temperature and pressure decrease continuously towards a calorically perfect, thermal equilibrium flow.

## 5. FADS least-squares solver

To verify the correct implementation of the pressure model in all of the subroutines, synthetically produced 'perfect' pressure distributions were fed to the least-squares solver. The original inputs to the pressure model (airflow angles, Mach, total pressure) were indeed perfectly retrieved. This was done at a typical Longshot condition, i.e. Mach number14 and total pressure close to 1 bar.

To verify the correct implementation of the least squares solver, next the synthetic pressure distribution was perturbed artificially in a range of ± 3%. These were then fed into the solver, together with the original inputs to the pressure model as an initial guess. In the case of convergence, the solver results typically look like in Fig. 14. The solver accurately retrieves the airflow angles and total pressure corresponding to the perturbed pressure distribution (red line is

17

original input condition). However, the reconstructed Mach number suffers enormously from the perturbations in the pressure distributions.
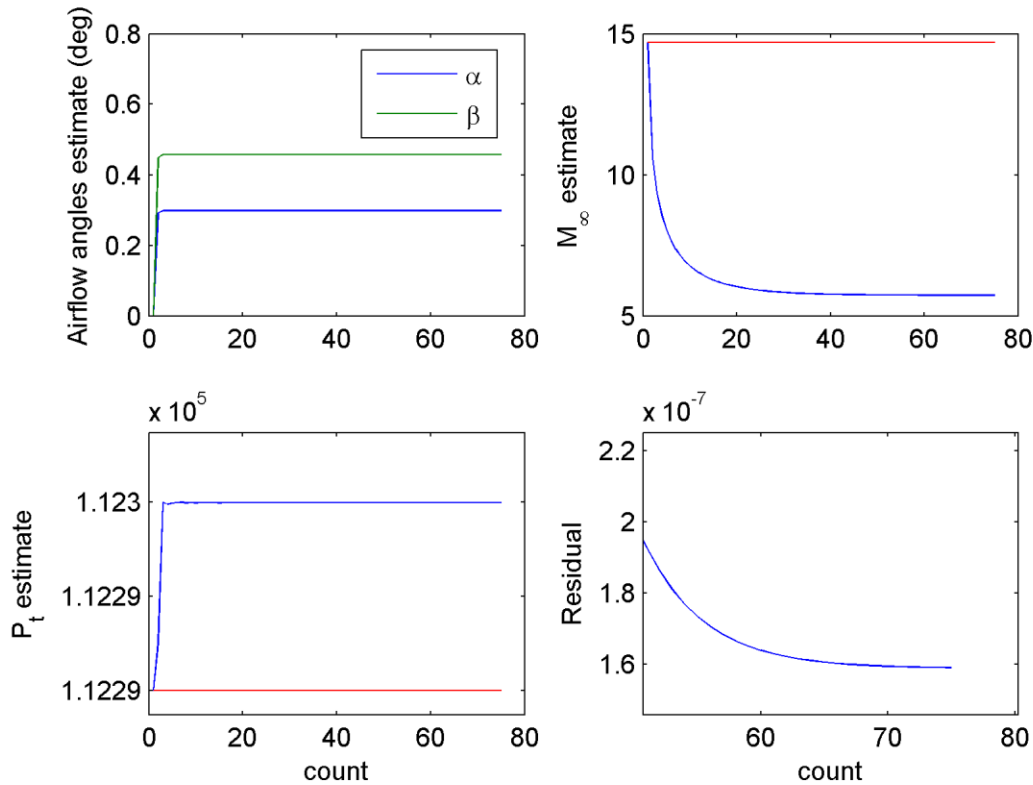


**Fig. 14 Solver convergence with perturbed synthetic data (single realization)**

In about half of one thousand realizations of this numerical experiment, the Mach number diverged. This has limited effects on the airflow angles and total pressure, but would prevent us from accurately calculating the dynamic pressure and hence the density. We believe this is both due to ill numerical conditioning, which could be compensated for in the future, and the limited number of off-stagnation-point pressure taps. The Mach number (or static pressure, if chosen to solve for that quantity), is derived from the pressure slope away from the stagnation point. In our five port cross layout, that slope is represented by only two pressure taps along a direction away from the stagnation point. More ports, preferably far away from the stagnation point, would improve Mach reconstruction.

## 6. Blunt probe testing in Longshot wind tunnel

At the moment we have performed tests 1-4 of the test matrix. Pressure and heat flux signals were obtained, and then fed to the least squares solver to reconstruct flow angles and total pressure. The Mach number was not reconstructed due to the shortcomings of the solver mentioned above. On the other hand, performance for reconstructing airflow angles and total

18

pressure is very good. The Mach number was constrained in a range about the initial guess, and this had no effect on the reconstructed flow angles or total pressure.

Fig. 15 and 16 show the pressure signals and pressure coefficients measured on the blunt probe in test 3. Off-stagnation points should measure the same pressures at zero total angle of attack. The on stagnation point measurement should match the value measured by the routine stagnation probe used for tunnel rebuilding (*Pt2a*, blue).
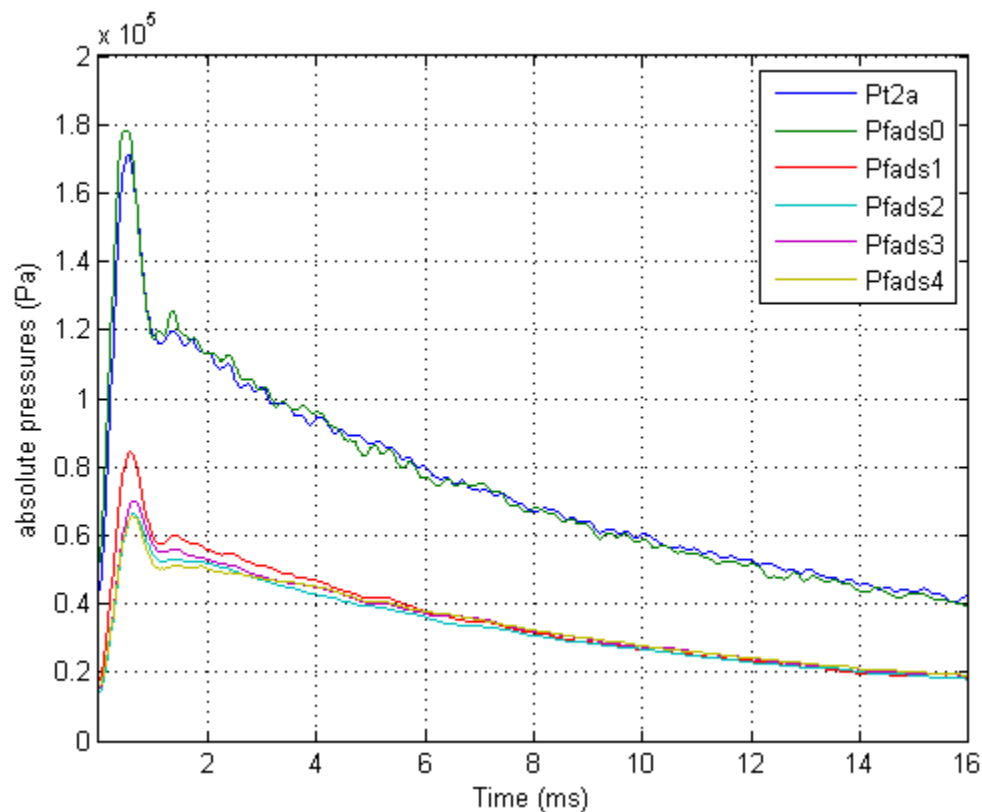


**Fig. 15 Absolute pressures on the blunt probe (test 3)**
**also shown: routine tunnel stagnation pressure measurement (Pt2a, blue)**

19
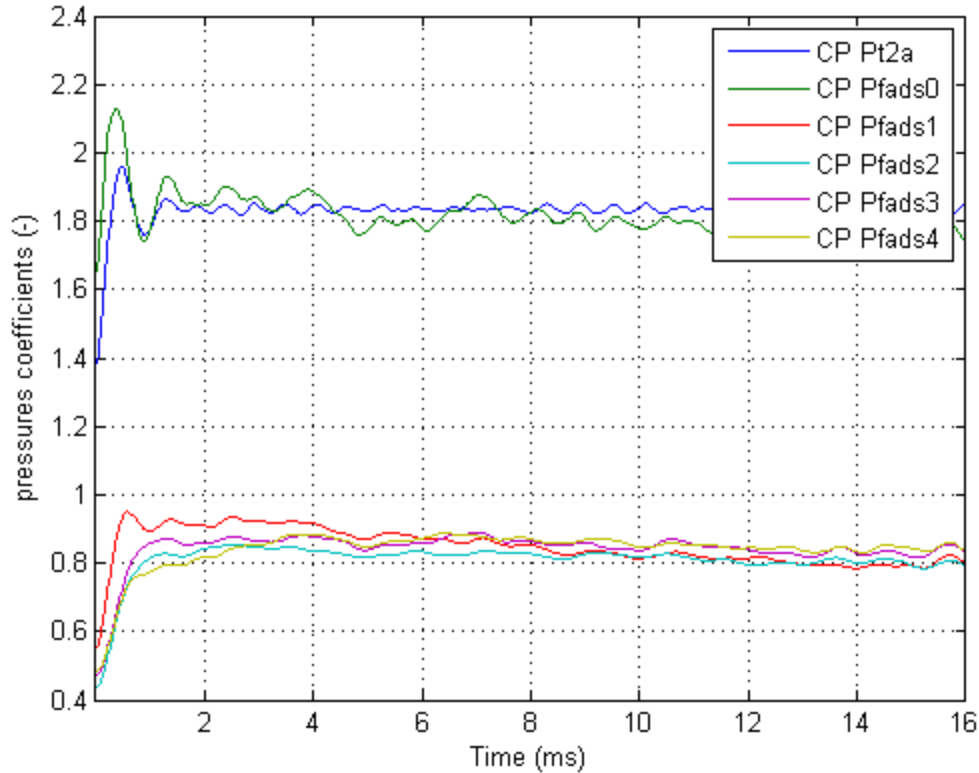
**Fig. 16 Pressure coefficients on the blunt probe (test 3)**
**also shown: routine tunnel stagnation pressure measurement (Pt2a, blue)**

Next, we reconstructed the angle of attack and sideslip in the wind tunnel frame using the FADS least square solver routine (Fig. 17-18) for all four tests. In the first milliseconds of the test, we see a strong transient response in both pitching and yawing. This seems to be due to probe movement, because rolling the probe by 180º in test 4 results in opposite pitching and yawing excursions in the wind tunnel reference frame. The transient response lasts for 1 ms in the pitching plane and 4 ms in the yawing frame. This may correspond to response frequencies of the support in different directions.

After the initial transient, the angle of attack then increases steadily from a negative value of about -1º to a steady value of between 0º and 1º in all four tests. The steady value is reached at 8 ms or half way through the test. These trends are independent of roll angle, suggesting flow misalignment. The bank angle maintains a steady value after the initial transient. In this case there is a clear difference between the fourth test at 180º roll angle and the others, indicating probe yaw misalignment in the first three tests.

20
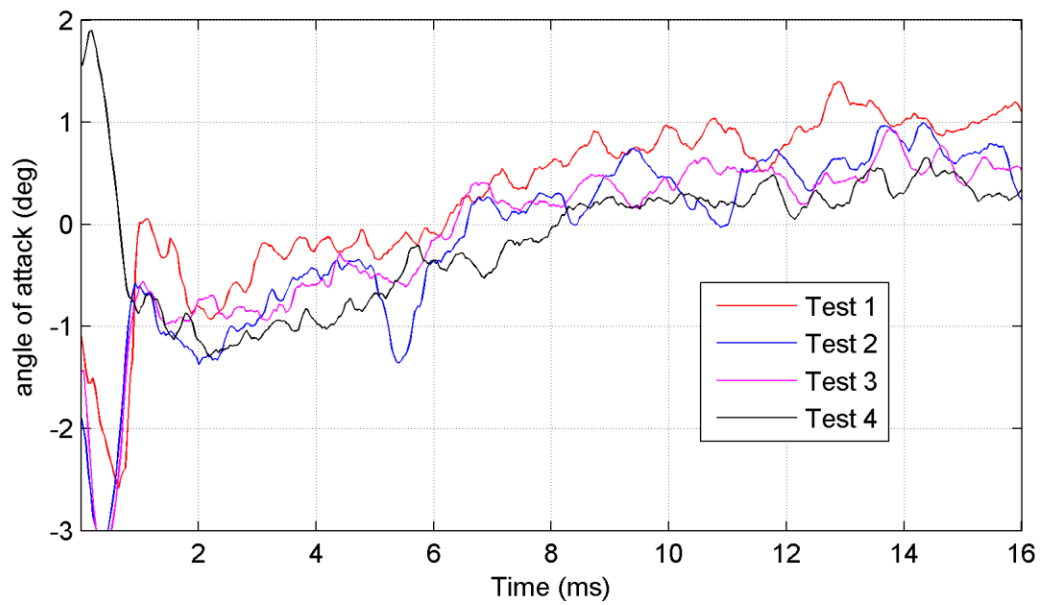
**Fig. 17 FADS reconstructed angle of attack in wind tunnel reference frame**
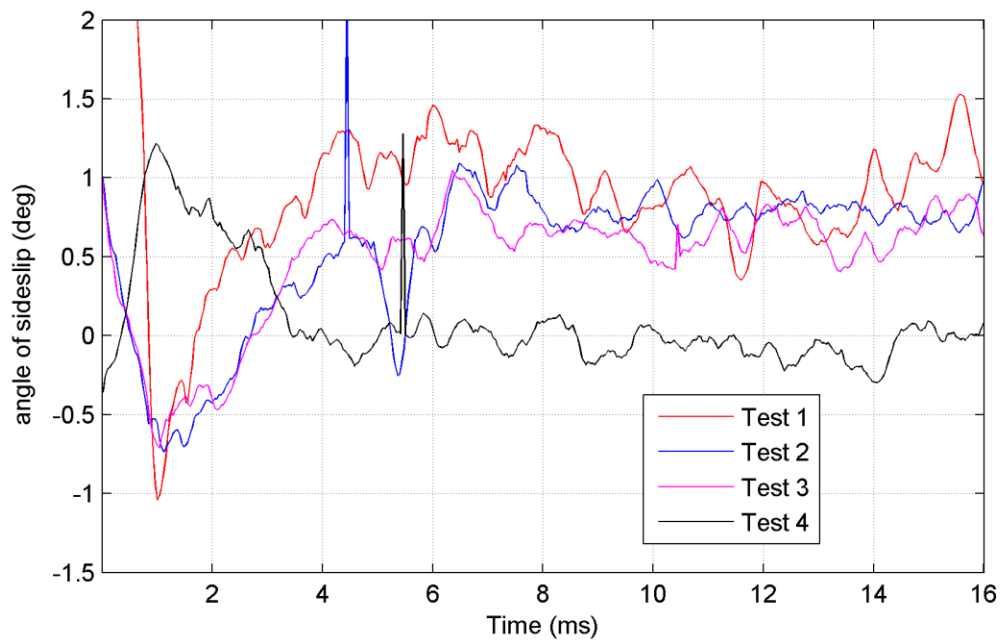


**Fig. 18 FADS reconstructed angle of sideslip in wind tunnel reference frame**

21
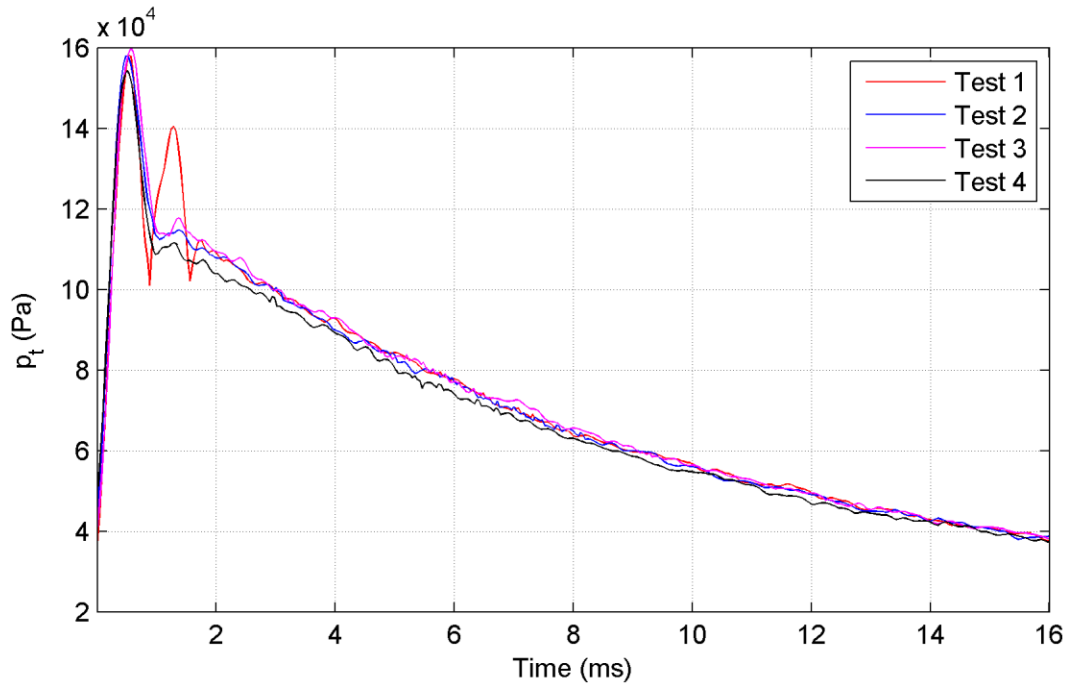
**Fig. 19 FADS reconstructed stagnation pressure**

The least-squares reconstructed total pressures shown in Fig. 19 are very consistent with the center pressure tap signal, but less with the routine tunnel stagnation pressure measurements which were up to 3% higher in all tests (not shown). At this point it is not clear whether this is due to sensor error or the different diameters of the two probes (25 mm versus 100 mm). As mentioned before, the Mach angles could not be reconstructed successfully from the measurements due to the solvers sensitivity to noise.
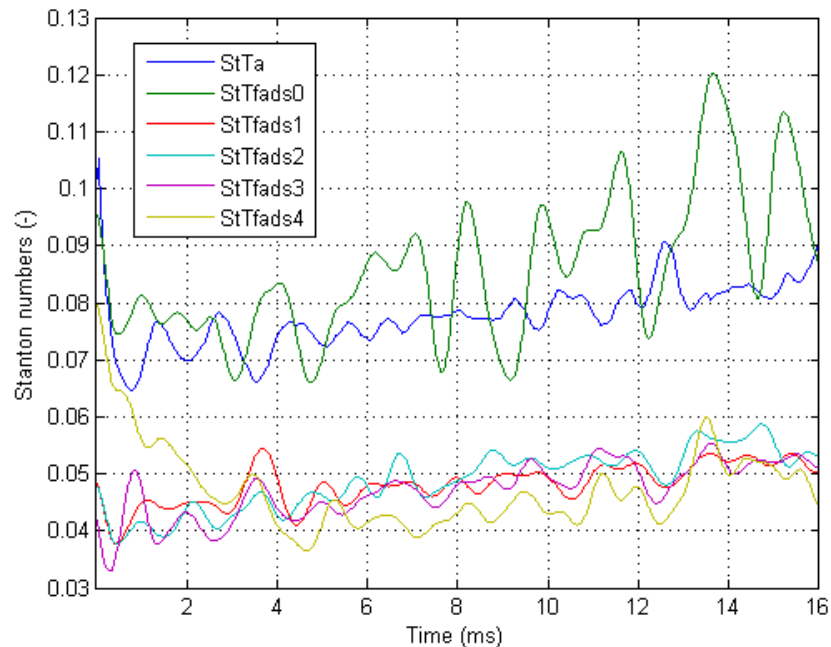


**Fig. 20 blunt probe heat flux signals (Stanton number) normalized to account for radius (test 3)**

22

Finally, Fig. 20 shows the heat flux at the various blunt probe measurement locations, compared to the routine stagnation point tunnel measurement (*StTa*, blue). The heat flux is expressed as the Stanton number, additionally normalized by the square root of the probe curvature radius. In all four tests, the stagnation point heat flux was quite noisy on the blunt probe. This could be remedied in the future by cleaning the thermocouple junction from which the heat flux is inferred. More importantly, there seems to be a 10% deviation between the routine tunnel measurement and the blunt probe stagnation heat flux in the second half of the test.

# V. Conclusion

We have developed a high temperature 1-D solver to reconstruct the Longshot wind tunnel conditions. It supports calorically imperfect, thermally perfect flows in thermal equilibrium or non-equilibrium. For non-equilibrium in the Longshot, the vibrational temperature has to be imposed. We obtained a prediction by solving Vibrational-Translational Energy Transfer and energy conservation equations for the Longshot nozzle geometry. Compared to the traditional rebuilding method, thermal non-equilibrium has a strong effect on the reconstructed density and Mach number of up to 6% and 4% respectively. Caloric imperfection had a more limited effect of up to 1% and 0,4% respectively. These results indicate that better understanding of thermal non-equilibrium due to the strong nozzle expansion is required to use the wind tunnel as a FADS calibration tool. Specifically, prior knowledge of the vibrational temperature is required. Caloric imperfections need to be taken into account to reconstruct the flow conditions as well, but this requires no prior knowledge.

A multi-sensor static pressure 'Nagamatsu' probe was developed and manufactured to improve on earlier single sensor measurements that indicated higher than expected static pressure. The probe has been verified to be leak-free, but due to technical delays it has not been tested yet.

We have developed a FADS least squares solver to rebuild flow angles, total pressure and Mach number using a modified Newtonian flow model. It works well for flow angles and total pressure, but diverges on the Mach number when provided with wind tunnel data or strongly perturbed synthetic data. This shortcoming made it unable to reconstruct the Mach number in the wind tunnel tests of a blunt spherical probe. We should assess whether solving for other unknowns (i.e. static pressure and/or dynamic pressure) improves convergence behavior.

The blunt spherical probe was manufactured and equipped with both pressure and heat flux sensors. Utilizing only the pressure data at this point, the FADS solver reconstructed total pressure and flow angles. The total pressure differs from routine wind tunnel measurements by up to 3%, either due to sensor error or diameter effects. The flow angles were accurately reconstructed and revealed both probe and flow misalignment. After an initial transient seemingly due to probe motion, the sideslip angle stays constant but the angle of attack steadily increases until half way through the test. After that it remains constant at values between 0º and 1º regardless of probe roll angle. This suggests more investigation into flow alignment is required.

# VI. References

[1] Koppenwallner G. and Müller-Eigner R. Definitionsstudie anström- und ober-flachenusssonden für den verdünnten strömungsbereich, teil 2: Staudrucksonde. HTG Hyperschalltechnologie Göttingen, Rept. No. 92-15, 1992.

[2] NASA SP-219, Symposium Proceedings of 'Status of Passive Inflatable Falling-Sphere Technology for Atmospheric Sensing', Langley Research Center, September 23-24 1969.

[2] Brent R. Cobleigh, Stephen A. Whitmore, and Edward A. Hearing. Flush airdata sensing (fads) system calibration procedures and results for blunt forebodies. NASA TP-1999-209012, 1999.

[3] Short Course on Uncertainty Quantification, 15-16 April 2011, Stanford University, California, and 13-14 May 2011, Bruges, Belgium, Uncertainty quantification in computational fluid dynamics, 24-28 October 2011, RTO-AVT-193 VKI Lecture Series, T. Magin and G. Iaccarino, von Karman Institute for Fluid Dynamics, Rhode-St-Genèse, Belgium, 2011.

[4] H. Olivier and P. zur Nieden. Determination of atmospheric densities from re-entry flight data. Journal of spacecraft and rockets, VOL. 44:No. 2, March-April 2007.

[5] B. Bottin. Aerothermodynamic Model of an Inductively-Coupled Plasma Wind Tunnel, PhD thesis, von Karman Institute For Fluid Dynamics, 1991.

[6] W. G. Vincenti and Charles H Kruger, Introduction to Physical Gas Dynamics, 1965.

[7] T. E. Magin. A Model for Inductive Plasma Wind Tunnels. PhD thesis, Universite Libre de Bruxelles, 2004.

[8] Nagamatsu H.T., R.E. Geiger, R.R. Sheer, Real gas effects in flow over blunt bodies at hypersonic speed, Journal of Aeronautical Science, Vol. 27, No. 4, pp. 241-251, 1960.

[9] J. D. Anderson Jr. Hypersonic and High-Temperature Gas Dynamics Second Edition, American Institute of Aeronautics and Astronautics, Inc., 2006.

[10] F. R. Riddell and J. A. Fay, Theory of stagnation point heat transfer in dissociated air, J. of the Aeronautical Sciences, Vol. 25, pp. 73-85, 1958.

[11] I.A. Johnston, Simulation of Flow Around Hypersonic Blunt Nosed Vehicles for the Calibration of Air Data Systems, Dept. of Mechanical Engineering, University of Queensland, PhD thesis, 1999.

[12] C. D. Karlgaard, Roger E. Beck, Stephen A. O'Keefe, Paul M. Siemers, and Brady A. White. Mars entry atmospheric data system modeling and algorithm Development. NASA Technical Reports Server (NTRS), AIAA Paper 2009-3916; LF99-8954, 2009.

# VII. Appendix

**Po, Pt2,Q(ref) measured**
**Initial guess: 2000 < To < 2500 K**

**calculation of Toperf et Poperf**
$\rho o = f(Po, To)$ ⎫ Hirschfelder
$so = f(To, \rho o)$ ⎬ equation of state
$ho = f(To, Po, \rho o)$ ⎭
(hoperfect gas = horeal gas)
(soperfect gas = soreal gas)
Toperf = ho/Cp

$$Poperf := \exp\left(\frac{So^0}{R} - \frac{so}{R} - \frac{Cp}{R} \cdot \ln(Toperf)\right) \,_*$$

**calculation of Tt2**

$$\frac{T0perf}{Tt2} := 0.9749 + (4.30610)^5 \cdot T0perf + 1.9610^{-8} \cdot T0perf^2 - 5.2810^{-12} \cdot T0perf^3 \,_*$$

**Calculation of Mach number**

$$\frac{Pt2}{P0perf} := \left[\frac{(\gamma + 1) \cdot M^2}{(\gamma - 1) \cdot M^2 + 2}\right]^{\frac{\gamma}{\gamma - 1}} \cdot \left[\frac{\gamma + 1}{2 \cdot \gamma \cdot M^2 - (\gamma - 1)}\right]^{\frac{1}{\gamma - 1}} \,_*$$

calculation of infinite conditions:
$P\infty, T\infty, \rho\infty, U\infty$
Reynolds: Re

$$Ti := \left[To \cdot \left(1 + \frac{\gamma - 1}{2} \cdot M^2\right)\right]^{-1}, \quad Pi := \left[Po \cdot \left(1 + \frac{\gamma - 1}{2} \cdot M^2\right)\right]^{\frac{\gamma}{1 - \gamma}}, \quad \rho i := \frac{Pi}{r \cdot Ti} \,_*$$

$$Ui := \frac{M}{\sqrt{\gamma \cdot r \cdot T}} \,_*, \quad Re_{Xlref} := \frac{\rho_\infty \cdot U_\infty}{\mu_\infty} \cdot Xlref \,_*$$

Use Fay-Riddell equation
for **calculation of Qt2**
Qt2: heat flux at the
stagnation point

$$Qt2 := 0.768 Pr^{-0.6} \cdot \left(\frac{Pt2}{r \cdot Tamb} \cdot \mu w\right)^{0.1} \cdot \left(\frac{Pt2}{r \cdot Tt2} \cdot \mu t2\right)^{0.4} \cdot (Ht2 \cdot r \cdot Tt2 - hw) \cdot (2 \cdot r \cdot Tt2)^{0.25} \,_*$$

Keyes' viscosity law

Qt2=Q(ref) —— yes —— ● END

no

New To

26